Author/s:
Zavras, A;Krstic, M;Dugourd, P;Bonacic-Koutecky, V;O'Hair, RAJ

Title:
Selectivity Effects in Bimetallic Catalysis: Role of the Metal Sites in the Decomposition of Formic Acid into H-2 and CO2 by the Coinage Metal Binuclear Complexes [dppmMM(H)](+)

Date:
2017-04-07

Citation:
Zavras, A., Krstic, M., Dugourd, P., Bonacic-Koutecky, V. & O'Hair, R. A. J. (2017). Selectivity Effects in Bimetallic Catalysis: Role of the Metal Sites in the Decomposition of Formic Acid into H-2 and CO2 by the Coinage Metal Binuclear Complexes [dppmMM(H)](+). ChemCatChem, 9 (7), pp.1298-1302. https://doi.org/10.1002/cctc.201601675.

Persistent Link:
https://hdl.handle.net/11343/292608

Title: Selectivity Effects in Bimetallic Catalysis: Role of the Metal Sites in the Decomposition of Formic Acid into H2 and CO2 by the Coinage Metal Binuclear Complexes [dppmMM'(H)]+

Authors: Athanasios Zavras; Marjan Krstić; Philippe Dugourd; Vlasta Bonačić-Koutecký; Richard A J O'Hair, PhD DSc

To be cited as: 10.1002/cctc.201601675

Link to VoR: https://doi.org/10.1002/cctc.201601675

Selectivity Effects in Bimetallic Catalysis: Role of the Metal Sites in the Decomposition of Formic Acid into H_2 and CO_2 by the Coinage Metal Binuclear Complexes $[dppmMM'(H)]^+$

Athanasios Zavras,[a] Marjan Krstić,[b] Philippe Dugourd,[c] Vlasta Bonačić-Koutecký*[b,d] and Richard A. J. O'Hair*[a]

Abstract: Design of new bimetallic catalysts requires an understanding of how cooperative effects of the metal sites influences reactivity. Here we show how switching one or both of the silver atoms in binuclear silver hydride cations, $[dppmAg_2(H)]^+$, with all combinations of copper and/or gold maintains selective dehydrogenation of formic acid while enhancing reactivity by up to 2 orders of magnitude. This is a key step in the selective, catalyzed extrusion of carbon dioxide from formic acid, HO_2CH, with important applications in hydrogen storage and in situ generation of H_2. Decarboxylation of $[dppmMM'(O_2CH)]^+$ via collision induced dissociation regenerates $[dppmMM'(H)]^+$. DFT calculations provide insights into these cooperative effects. The copper homobinuclear catalyst performs best overall.

Introduction

Catalytic cooperative effects are ubiquitous in nature and in synthetic systems.[1] The requirement for two metals, either of the same element or of two different elements, to complete a catalytic cycle represents an important synergistic effect[2] in both heterogeneous[3] and homogenous catalysis[4,5] and has been termed ***bimetallic catalysis***.[3-5] While single site homogenous catalysis represents an attractive way of "bottom-up" design of catalysts, the design principles for bimetallic catalysis are still not well understood. In cases where reactivity is catalytic in one metal and stoichiometric in the other metal, transmetallation can be the crucial step for a successful catalytic cycle.[4] Catalysts that contain two metal sites are attractive candidates for developing a deeper understanding of bimetallic catalysis since they allow the role of the ligand and each of the metal centres to be examined.[5] By using multistage mass spectrometry techniques[6] to study these systems in the gas-phase[7] it is possible to examine the role of each metal centre on the elementary steps of a catalytic cycle involving homo- and heteronuclear clusters.[8]

As one of the few organic liquids with potential for hydrogen storage applications, formic acid has attracted the attention of the catalysis community.[9] In the absence of a catalyst, high temperatures are required for the gas-phase decarboxylation of formic acid (eq. 1), which is in competition with dehydration (eq. 2).[10] Thus there has been considerable interest in developing metal catalysts to selectively decarboxylate formic acid at low temperatures.[11]

$$HCO_2H \rightarrow H_2 + CO_2 \quad (1)$$

$$\rightarrow H_2O + CO \quad (2)$$

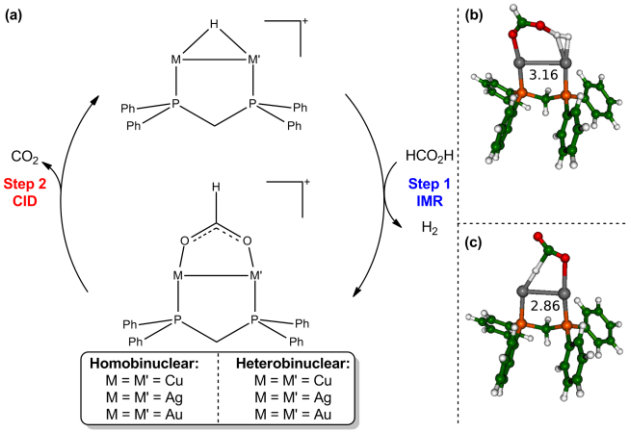

Figure 1. Selective decarboxylation of formic acid. (a) Two step catalytic involving bimetallic catalysis. DFT calculations highlight the role of both metal centers for: (b) Transition state (TS) for dehydrogenation of formic acid for $[dppmAg_2H]^+$.[12] (c) TS for decarboxylation for $[dppmAg_2(O_2CH)]^+$.[12]

[a] Mr. A, Zavras, Prof. R. A. J. O'Hair,
School of Chemistry and Bio21 Molecular Science and Biotechnology Institute
University of Melbourne
30 Flemington Rd, Parkville, Victoria 3010 (Australia)
E-mail: rohair@unimelb.edu.au
[b] Mr. M. Krstić, Prof. V. Bonačić-Koutecký
Interdisciplinary Center for Advanced Sciences and Technology (ICAST), University of Split
Meštrovićevo Šetalište 45, 21000 Split (Croatia)
[c] Prof. P. Dugourd,
Institut Lumière Matière, UMR5306 Université Lyon 1-CNRS
Université de Lyon
5 rue de la Doua, 69622 Villeurbanne (France)
[d] Prof. V. Bonačić-Koutecký
Chemistry Department
Humboldt University of Berlin
Brook-Taylor-Strasse 2, 12489 Berlin (Germany)

Supporting information for this article is given via a link at the end of the document.

We recently showed that the choice of ligand is crucial to developing a two-step catalytic cycle for the selective extrusion of carbon dioxide from formic acid by $[dppmAg_2(H)]^+$ in the gas phase (Figure 1).[12] The bis(diphenylphosphino)-methane (dppm) ligand was found to reshape the geometry of the binuclear $Ag_2(H)^+$ scaffold, thereby switching on dehydrogenation to produce $[dppmAg_2(O_2CH)]^+$ and H_2 (Fig 1a, Step 1). Decarboxylation of $[dppmAg_2(O_2CH)]^+$ via collision induced dissociation (CID) regenerates $[dppmAg_2(H)]^+$ (Fig 1a, Step 2). Both silver sites are involved in the crucial transition states for dehydrogenation and decarboxylation, with one acting as an "anchor" for the oxygen of formic acid (step 1, Fig 1b) or the coordinated formate (step 2, Fig 1c) while the other triggers dehydrogenation or hydride transfer. The stoichiometry of the metal complex is crucial for this catalytic cycle, with $[L_2Ag_2(H)]^+$, $[L_2Ag_4(H)_3]^+$, $[L_2Ag_4(O_2CH)(H)_2]^+$ and $[L_2Ag_4(O_2CH)_2(H)]^+$ being unreactive towards HCO_2H.[13]

Here we use MS experiments and DFT calculations to examine the chemistry of all of the related homo- and heterobinuclear complexes $[dppmMM'(H)]^+$ of the d^{10} coinage metals where M or M' = Cu, Ag and Au.[14] This allows an evaluation of how cooperative effects between the metal centers influence both steps of the catalytic cycle.

Results and Discussion

Formation of $[dppmMM'(H)]^+$.

Our entry into the catalytic cycle was via the coordinated formates, $[dppmMM'(O_2CH)]^+$, which were transferred to the gas-phase via electrospray ionization (ESI) of a 50 µM acetonitrile solution containing a mixture of Cu_2O:Ag_2O:$AuClPPh_3$ (1:1:2) to which 10 equivalents of formic acid was added (Supporting information Figure S1a and related discussion). All homo and hetero binuclear formates were formed from this solution, as confirmed via their isotope patterns (Figure S1b) and high-resolution mass spectrometry (HRMS) experiments (Figure S2). The HRMS experiments also identified the presence of isobaric impurities for $[dppmAu_2(O_2CH)]^+$ (*m/z* 823, Figure S2b), $[dppmCuAu(O_2CH)]^+$ (*m/z* 689, Figure S2d), and $[dppmAgAu(O_2CH)]^+$ (*m/z* 733, Figure S2e). CID (MS^2) of the mass-selected formate complexes, $[dppmMM'(O_2CH)]^+$ (Figure S3), generated abundant hydride complexes $[dppmMM'(H)]^+$ via decarboxylation with the exception of $[dppmAu_2(H)]^+$ (*m/z* 779, Figure S3b) and $[dppmAgAu(H)]^+$ (*m/z* 689, Figure S3e). The elemental composition of each of the hydride complexes generated via the decarboxylation of the coordinated formates (Figure 1a, Step 2) was confirmed by HRMS (Figure S4). Subsequent mass-selection provided hydride complexes devoid of any isobaric impurities for ion-molecule reactions with formic acid in a series of MS^3 experiments.

Step 1 of the catalytic cycle: Ion-molecule reactions between $[dppmMM'(H)]^+$ and formic acid.

All hetero- and homobimetallic hydride complexes react with formic acid to regenerate the formate complex $[dppmMM'(O_2CH)]^+$ (Figure 1a, Step 1 and Figure 2). To evaluate the roles of the metal centers on reactivity, the temporal decay of the reactant ion, $[dppmMM'(H)]^+$, was monitored over a range of activation times and concentrations of formic acid (Figure S5) to yield rate constants, which when compared to the predicted collision rates gave the reaction efficiencies listed Table 1.[17] The experimentally observed reactivity order follows: $[dppmAu_2(H)]^+$ ≈ $[dppmCu_2(H)]^+$ > $[dppmCuAu(H)]^+$ ≈ $[dppmCuAg(H)]^+$ >> $[dppmAgAu(H)]^+$ ≈ $[dppmAg_2(H)]^+$ with a ca. 2 orders of magnitude difference in reactivity between the most and least reactive complexes.

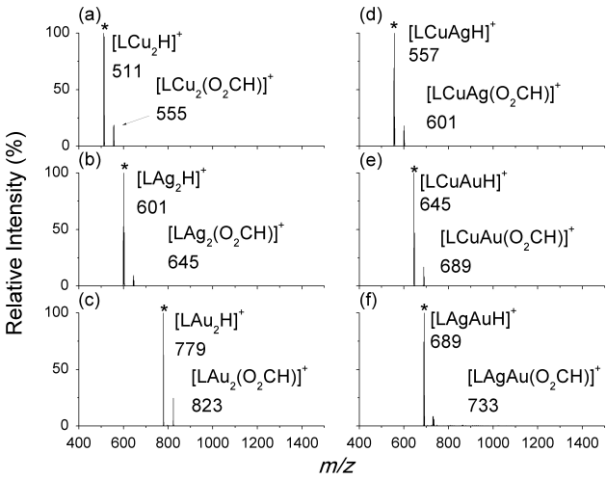

Figure 2. MS^3 LTQ spectra obtained in a 2D linear-ion trap at ≈ 298 K showing the ion-molecule reaction of formic acid with mass-selected hydrides, $[LMM'H]^+$ (L=dppm) for: **a,** M=M'=Cu, Activation time = 60 ms, $[HO_2CH]_{ion\ trap}$ = 2.24 x 10^9 molecules.cm^{-3}, **b,** M=M'=Ag, Activation time = 1000 ms, $[HO_2CH]_{ion\ trap}$ = 4.75 x 10^9 molecules.cm^{-3}, **c,** M=M'=Au, Activation time 20 ms = , $[HO_2CH]_{ion\ trap}$ = 2.24 x 10^9 molecules.cm^{-3}, **d,** M=Cu;M'=Ag, Activation time = 30 ms, $[HO_2CH]_{ion\ trap}$ = 3.72 x 10^9 molecules.cm^{-3}, **e,** M=Cu;M'=Ag Activation time = 50 ms, $[HO_2CH]_{ion\ trap}$ = 8.19 x 10^9 molecules.cm^{-3}, and **e,** M=Ag;M'=Au Activation time = 1000 ms, $[HO_2CH]_{ion\ trap}$ = 8.96 x 10^8 molecules.cm^{-3}. A * represents the mass-selected precursor ion. The most intense peak in the cluster is represented by the *m/z* value.

Table 1. Rates of ion-molecule reactions between $[LMM'(H)]^+$ and formic acid (L = dppm).

Reactant ion	k_{expt} [a,b,c]	Reaction efficiency (φ) [d]	DFT E_{act} (eV) calculated [f]
$[LCu_2(H)]^+$	1.20±0.01x10^{-9}	113.6±6.1	-0.66 (0.07)
$[LAg_2(H)]^+$	1.53±0.03x10^{-11}	1.4±0.1	-0.06 (0.18)
$[LAu_2(H)]^{+[e]}$	1.47±0.09x10^{-9}	141.0±9.2	-1.02 (0.06)
$[LCuAg(H)]^+$	3.31±0.2x10^{-10}	31.5±2.1	-0.25 (0.47)
$[LCuAu(H)]^+$	4.51±0.4x10^{-10}	43.1±4.1	-0.3 (0.74)
$[LAgAu(H)]^+$	3.33±0.3x10^{-11}	3.2±0.3	-0.08 (0.18)

[a] Mean ± standard deviation (n=3). [b] In units of cm^3.$molecules^{-1}$.s^{-1}. [c] Rates for the reaction with formic acid with $[LMM'H]^+$ to regenerate $[LMM'(O_2CH)]^+$ as the product. Rates were determined by monitoring the decay of the reactant ion with a known concentration of formic acid over time. [d] Reaction efficiency (φ) = (k_{expt}/k_{ADO}) x 100. The k_{ADO} is the theoretical ion-molecule collision rate constant obtained from the average-dipole orientation (ADO) theory,[15] which was calculated using the Colrate program.[16] [e] data from ref [12]. [f] E_{act} relative to separated reactants (or relative to initial complex).

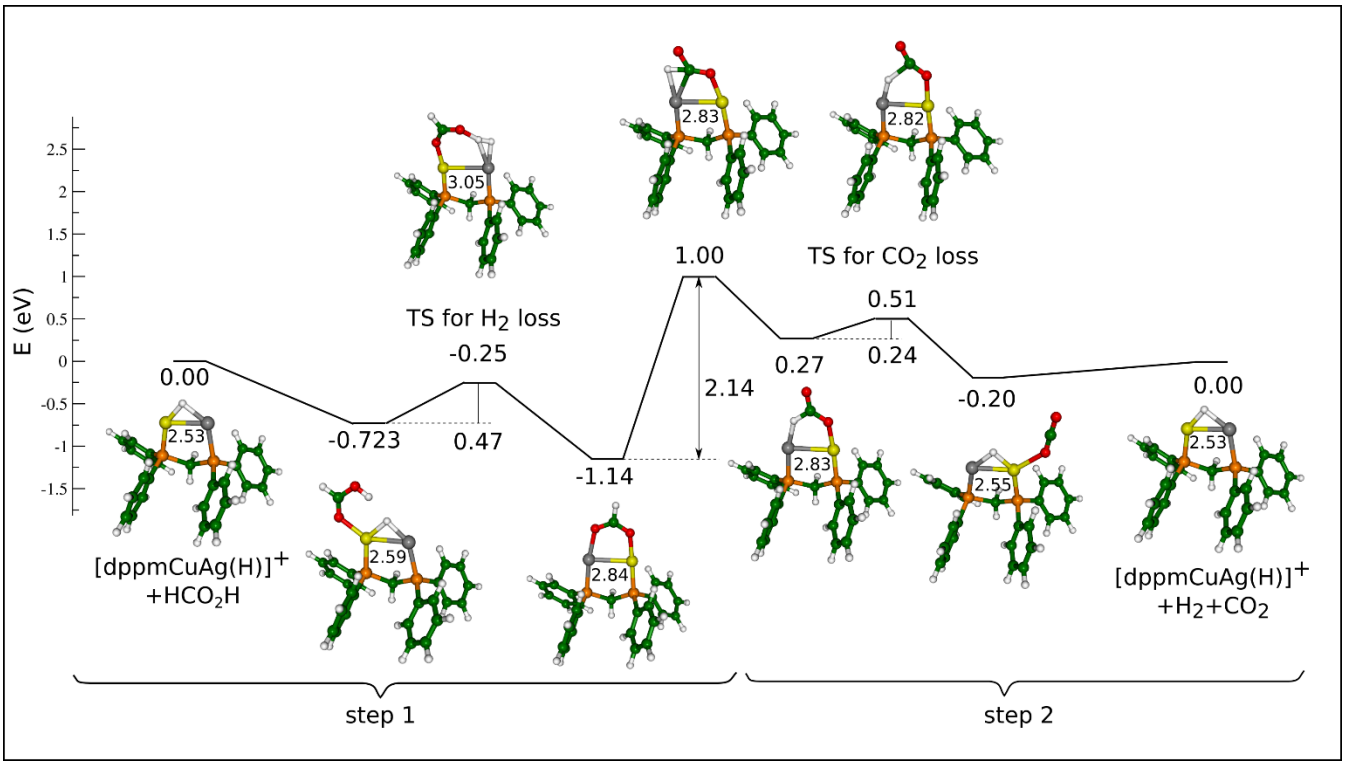

Figure 3. DFT-calculated energy profile for the preferred site of reactivity of the heterobinuclear complex for the two reaction steps in the catalytic cycle of Fig. 1a. Step 1: ion-molecule reaction of formic acid with $[dppmCuAg(H)]^+$ at the copper site; step 2: CID decarboxylation of $[dppmCuAg(O_2CH)]^+$ with hydride transfer to the silver site. Relative energies are in eV. All structures were fully optimized using DFT method with the hybrid B3LYP functional and def2-TZVP atomic basis set which has been used for all atoms. Silver atoms have been treated by Stuttgart relativistic effective core potential (RECP) with corresponding AO basis set. Silver = Ag, Yellow = Cu.

Step 2 of the catalytic cycle: CID of $[dppmMM'(O_2CH)]^+$ to regenerate $[dppmMM'(H)]^+$.

We next examined the ease of decarboxylation (Step 2, Figure 1). Due to the presence of isobaric impurities from ESI/MS as discussed previously, the formate complexes formed via ion-molecule reactions between the hydrides and formic acid (Step 1), were mass-selected and allowed to undergo CID in a MS^4 experiment (Figure S6). This precluded energy resolved CID measurements of thresholds for decarboxylation. In all cases decarboxylation was the major fragmentation pathway (Scheme S1), with competing formation of $[dppmM]^+$ and/or $[dppmM']^+$ being minor channels. At a normalized collision energy of 15% and an activation time of 10 ms, the amount of hydride formed (relative to all ions present in the CID spectrum) via decarboxylation follows the order of: $[dppmAg_2(O_2CH)]^+$ (88.6%) ≈ $[dppmCu_2(O_2CH)]^+$ (85%) > $[dppmCuAu(O_2CH)]^+$ (76.6%) ≈ $[dppmCuAg(O_2CH)]^+$ (76.5%) > $[dppmAgAu(O_2CH)]^+$ (45%) > $[dppmAu_2(O_2CH)]^+$ (28.1%).

DFT calculations on the mechanisms and energetics of both steps associated with the catalytic cycle.

The DFT calculated energy diagrams are largely consistent with the experiments and provide insights into how reactivity is modulated by the nature of the metal centers (Figure 3 and Supporting Information Figures S8-S11).

Step 1 of the catalytic cycle must be an exothermic process with barriers that lie below the separated reactants in order for it to occur under the near thermal conditions of the ion-trap.[18] Indeed this is the case, with the most exothermic reaction occurring for $[dppmCu_2(H)]^+$ (Table S2). In all cases an initial complex between the hydride, $[dppmMM'(H)]^+$, and formic acid is formed, which then proceeds via a single transition state to produce H_2 and the thermodynamically favoured O,O-bridged formate complex, $[dppmMM'(O_2CH)]^+$. In all cases this critical TS has a structure where one metal site acts as an "anchor" for the oxygen of the formic acid while the other metal site contains the hydride that reacts via dehydrogenation. We have carried out a Mulliken charge analysis of the precursor ions and their complexes with formic acid (Figure S12). With the exception of $[dppmCu_2(H)]^+$ and $[dppmCuAg(H)]^+$, all precursor ions have partial negative charges on the coordinated hydride and a partial positive charge at the metal center(s). For the initial complexes between the hydride, $[dppmMM'(H)]^+$, and formic acid, the oxygen atom of the coordinated formic acid has a negative charge, while the O-H has the expected (-)(+) dipole. Taken together, this suggest that these can be regarded as dehydrogenation reactions in which the coordinated hydride reacts with the acidic O-H proton of the formic acid. In the case of the homobinuclear complexes, the well depth associated with the formation of the initial complex follows the order $[dppmAu_2(H)]^+$ (-1.08 eV) > $[dppmCu_2(H)]^+$ (-0.73 eV) > $[dppmAg_2(H)]^+$ (-0.24 eV) and thus dictates the observed reactivity.[19] For the heterobinuclear complexes,

formic acid can approach either of the two different metal centres. A detailed examination of all possible reactant complexes and transition states for attack at both copper and silver was carried out for $[dppmCuAg(H)]^+$ (Supporting Information Table S2). The most favoured site of attack is at copper (Figure 3), consistent with the relative reactivity order for the homobinuclear complexes. For $[dppmCuAu(H)]^+$ the preferred site of reactivity is Cu (Figures S10), while for $[dppmAgAu(H)]^+$ it is Au (Figures S11). Overall, there is good agreement between theory and experiment, with the DFT predicted activation energies for step 1 being inversely related to the measured reaction efficiencies (compare columns 4 and 3 of Table 1).

In contrast, decarboxylation is endothermic as it requires energization of $[dppmMM'(O_2CH)]^+$ through multiple collisions with the helium bath gas during the CID process. The DFT calculations reveal that both metal centers play a role in the mechanism for CO_2 release, which involves two steps (Figure 3 and Figures S8-10), except for $[dppmAgAu(O_2CH)]^+$, which only requires a single transition state (Figures S11). The first step involves breaking one of the M-O bonds to isomerize the O,O- bridged formate to its O-bound form, and is the rate determining step except for $[dppmAg_2(O_2CH)]^+$ and $[dppmCuAu(O_2CH)]^+$. The next step involves decarboxylation, to give the O bound $[dppmMM'(H)(OCO)]^+$ complex, which then loses CO_2. For the heterobinuclear complexes, hydride transfer from the coordinated formate can occur to either metal centre. A detailed examination of all possible transition states and intermediates associated with hydride transfer to either copper or silver sites was carried out for $[dppmCuAg(H)]^+$ (Supporting Information Table S2). In step 2, the most favoured site of attack is at silver (Figure 3), consistent with both the experimentally determined relative reactivity order and DFT calculated energetics for the homobinuclear complexes.

Conclusions

In conclusion, the DFT calculations show that both metal centers play a role in both steps of the catalytic cycle. One metal site acts as an "anchor" for the oxygen of formic acid (step 1) or formate (step 2) while the other site facilitates dehydrogenation (step 1)[19] or hydride transfer during decarboxylation of the coordinated formate (step 2). Since each metal center may influence each step of a catalytic cycle in a different way, the overall preferred bimetallic catalyst is that which represents a compromise in reactivity for all steps as well as the cost of the metal. This is the case here, where the cheaper, earth abundant copper catalyst $[dppmCu_2(H)]^+$ is the second most reactive complex and is regenerated from $[dppmCu_2(O_2CH)]^+$ slightly less efficiently that the hydride from CID of $[dppmAg_2(O_2CH)]^+$.

Experimental Section

Mass spectrometry experiments: Gas-phase experiments on phosphine ligated bimetallic formate clusters, formed as discussed in the Supporting Information, were carried out using a Finnigan hybrid linear quadrupole Fourier transform ion-cyclotron resonance (LTQ FTICR) mass spectrometer modified to allow the study of IMR.[20] The unimolecular fragmentation/dissociation of mass-selected phosphine ligated bimetallic clusters occurred via CID using a normalized collision energy between 20 – 25% and an activation time of 30 ms. The CID isolation width was 5 – 8 *m/z* from the centre of the ion cluster distribution. IMRs were carried by delivering a measured concentration of formic acid into the helium bath gas.

DFT calculations: The extensive search for lowest energy structures and transitions states was performed using the hybrid B3LYP[21] functional with def2-TZVP atomic basis set for all atoms.[22] Silver and/or gold atoms were treated by the Stuttgart relativistic effective core potential (RECP) with the corresponding AO basis set.[23]

Potential interactions between the aromatic rings of the dppm ligand, raises the question of whether dispersion corrections within DFT are required. We have tested the influence of dispersion correction on the structural properties of $[dppmAg_2H]^+$ and $[dppmAg_2(O_2CH)]^+$ complexes by introducing D3 into the DFT.[24] Since the energy profile remained almost unchanged when single point B3LYP-D3 energy calculations were carried out for each reaction step of the catalytic cycle we have not used it for all profiles. The use of other functionals with high averaged accuracy such as TPSSh[25] and M062X[26] does not change the overall energy profiles.

Acknowledgements

We thank the ARC for financial support *via* grant DP150101388 (to RAJO and PD). AZ acknowledges the award of an Australian Postgraduate PhD Scholarship. The research leading to these results has received funding from the European Research Council under the European Union's Seventh Framework Programme (FP7/2007-2013 Grant agreement N°320659). VBK and MK acknowledge computational facilities of the supercomputer "Bura" at the Universtiy of Rijeka and SRCE at University of Zagreb as well as Prof. Miroslav Radman at MedILS and Split-Dalmatia County for kind support.

Keywords: Bimetallic catalysis • Formic Acid • Selective Decarboxylation • Mass spectrometry • DFT calculations

[1] J. I. van der Vlugt, *Eur. J. Inorg. Chem.* **2012**, 363–375.
[2] For a recent review on synergistic effects in isolated transition metal systems in the gas-phase, see: G. Niedner-Schatteburg, Cooperative Effects in Clusters and Oligonuclear Complexes of Transition Metals in Isolation, Struct. Bond., in press DOI: 10.1007/430_2016_11
[3] W. Yu, M. D. Porosoff, J. G. Chen, *Chem. Rev.* **2012**, *112*, 5780–5817.
[4] M. H. Pérez-Temprano, J. A. Casares, P. Espinet, *Chem. Eur. J.* **2012**, *18*, 1864–1884.
[5] N. P. Mankad, *Chem. Eur. J.* **2016**, *22*, 5822–5829.
[6] (a) R. A. J. O'Hair, *Chem. Comm.* **2006**, 1469–1481. (b) R. A. J. O'Hair, N. J. Rijs, *Acc. Chem. Res.* **2015**, *48*, 329–340. (c) R. A. J. O'Hair, *Pure. Appl. Chem.* **2015**, *87*, 391–404.
[7] For reviews on the use of MS to examine catalysis in the gas phase see: (a) D. K. Böhme, H. Schwarz, *Angew. Chem. Int. Ed*. **2005**, *44*, 2336–2354. (b) D. Schröder, *Acc. Chem. Res.* **2012**, *45*, 1521–1532. (c) H. Schwarz, *Isr. J. Chem.* **2014**, *54*, 1413–1431. (d) R. A. J. O'Hair, *Int. J. Mass Spectrom.* **2015**, *377*, 121–129.
[8] For examples of bimetallic reactivity in the gas-phase, see: (a) K. Koszinowski, D. Schröder, H. Schwarz, *J. Am. Chem. Soc.* **2003**, *125*, 3676–3677. (b) K. Koszinowski, D. Schröder, H. Schwarz, *ChemPhysChem* **2003**, *4*, 1233–1237. (c) K. Koszinowski, D. Schröder, H. Schwarz, *Organometallics* **2004**, *23*, 1132–1139. (d) H. Al Sharif, K. L. Vikse, G. N. Khairallah,

R. A. J. O'Hair, *Organometallics*, **2013**, *32*, 5416–5427. (e) G. N. Khairallah, G. R. da Silva, R. A. J. O'Hair, *Angew. Chem. Int. Ed*. **2014**, *53*, 10979–10983. (f) K. L. Vikse, A. Zavras, T. H. Thomas, A. Ariafard, G. N. Khairallah, A. J. Canty, B. F. Yates, R. A. J. O'Hair, *Organometallics*, **2015**, *34*, 3255–3263.

[9] (a) M. Grasemann, G. Laurenczy, *Energy Environ. Sci.*, **2012**, *5*, 8171-8181; (b) S. Enthaler, J. von Langermann, T. Schmidt, *Energy Environ. Sci.*, **2010**, *3*, 1207-1217.

[10] (a) K. Saito, T. Shiose, O. Takahashi, Y. Hidaka, F. Aiba, K. Tabayashi, *J. Phys. Chem. A*, **2005**, *109*, 5352–5357; (b) J.-G. Chang, H.-T. Chen, S. Xu, M. C. Lin, *J. Phys. Chem. A*, **2007**, *111*, 6789-6797.

[11] B. Loges, A. Boddien, F. Gärtner, H. Junge, M. Beller, *Topics Catal.*, **2010**, *53*, 902–914.

[12] A. Zavras, G. N. Khairallah, M. Krstić, M. Girod, S. Daly, R. Antoine, P. Maitre, R. J. Mulder, S.-A. Alexander, V. Bonačić-Koutecký, P. Dugourd, R. A. J. O'Hair, *Nature Communications,* **2016**, *7*, 11746.

[13] A. Zavras, J. M. White, R. A. J. O'Hair, *Dalton Trans.,* **2016**, *45*, 19408 - 19415.

[14] For a comprehensive review on the formation and reactions of coinage metal hydrides see: A. J. Jordan, G. Lalic, J. P. Sadighi, *Chem. Rev.* **2016**, *116*, 8318–8372.

[15] T. Su, M. T. Bowers, *Gas-Phase Ion Chemistry* **1949**.

[16] K. F. Lim, *Quantum Chemistry Program Exchange* **1994** *14*, 3. The program Colrate is available for download from the author's website at Deakin University, Geelong, Victoria, Australia: http://www.deakin.edu.au/~lim/programs/COLRATE.html.

[17] Several studies have highlighted that the measured rate constants of metal clusters can exceed the theoretical ADO rate constants, which use a point charge model, by up to a factor of 3–4: (a) O. P. Balaj, I. Balteanu, T. T. J. Rossteuscher, M. K. Beyer, V. E. Bondybey, *Angew., Chem., Int. Ed.* **2004**, *43*, 6519–6522. (b) M. L. Anderson, M. S. Ford, P. J. Derrick, T. Drewello, D. P. Woodruff, S. R. Mackenzie, *J. Phys. Chem. A* **2006**, *110*, 10992–11000.

[18] (a) S. Gronert, *J. Am. Soc. Mass Spectrom.*, **1998**, *9*, 845–848. (b) W. A. Donald, G. N. Khairallah, R. A. J. O'Hair, *J. Am. Soc. Mass Spectrom.*, **2013**, *24*, 811–815.

[19] Although there is a dearth of experimental thermochemical data for these systems, the DFT calculated binding energy orders are consistent with the relative atomic metal cation water binding energy orders: $D(H_2O\text{-}Au^+) > D(H_2O\text{-}Cu^+) > D(H_2O\text{-}Ag^+)$ (J. Roithová, D. Schröder*, Coord. Chem. Rev.* **2009**, *253*, 666).

[20] W. A. Donald, C. J. McKenzie, R. A. J. O'Hair, *Angew. Chem. Int. Ed*., **2011**, *50*, 8379–8383.

[21] A. D. Becke, *J. Chem. Phys.* **1993** *98*, 5648–5652.

[22] A. Schäfer, H. Huber, R. Ahlrichs, *J. Chem. Phys.*, **1994**, *100*, 5829–5835.

[23] D. Andrae, U. Haeussermann, M. Dolg, H. Stoll, H. Preuss, *Theor. Chim. Acta.*, **1990**, 77, 123–141.

[24] S. Grimme, J. Antony, S. Ehrlich, H. Krieg, *J. Chem. Phys.*, **2010**, *132*, 154104.

[25] J. Tao, J. P. Perdew, V. N. Stavorevov, G. E. Scuseria, *Phys. Rev. Lett.*, **2003**, *91*, 146401.

[26] Y. Zhao, D. G. Truhlar, *Theor. Chem. Acc.*, **2008**, *120*, 215-241.

Entry for the Table of Contents

Bimetallic coinage metal hydrides react with formic acid to liberate hydrogen. By systematically changing the metal centres reactivity trends have been established. The reaction efficiency can be increased by up to 2 orders of magnitude.

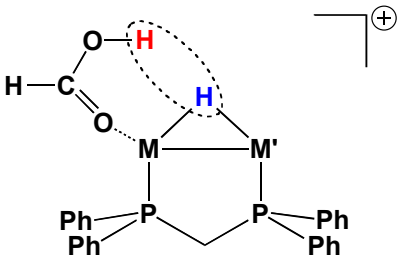

Reactivity order for dehydrogenation:
$[dppmAu_2(H)]^+ \approx [dppmCu_2(H)]^+ >$
$[dppmCuAu(H)]^+ \approx [dppmCuAg(H)]^+ >>$
$[dppmAgAu(H)]^+ \approx [dppmAg_2(H)]^+$